

# Application of Random Fields and Polynomial Chaos Expansions to Slope Reliability Analysis

Joana-Sophia Levkov

*Graduate Student, Dept. of Civil Engineering, Ecole Polytechnique Fédéral de Lausanne, Lausanne, Switzerland*

Gil Jacot-Descombes

*Civil Engineer, GeoMod SA Lausanne, Switzerland*

Stéphane Commend

*Professor at HES-SO, University of Applied Sciences Western Switzerland, Fribourg, and Civil Engineer at GeoMod SA Lausanne, Switzerland*

**ABSTRACT:** This paper aims to find the difference between two types of probabilistic slope stability analysis under a rainfall event. The first admits a uniform soil and takes into account uncertainty of the soil properties. The second includes spatial variability of the soil properties. Both analyses are performed using a Monte Carlo framework with the help of a meta-model, in particular a Polynomial Chaos Expansion (PCE). The PCE is built based on 2D finite element realisations and allows a quick evaluation of new ones. This provides an efficient reliability analysis when performing the Monte Carlo Simulation method. A comparison between the probabilities of failure between the two approaches is shown. Furthermore, the effect of the correlation lengths of the random field on the probabilities of failure is evaluated.

## 1. INTRODUCTION

One great challenge in geotechnical engineering is the correct definition of soil parameters when it comes to numerical simulation by the finite element method. They are often deduced from a limited number of in situ soil measurements. However, these measurements are expensive and only provide local information about the soil. Yet its mechanical properties vary naturally within the geometric body. To account for this spatial variability, the use of random fields based on geostatistical inputs has been recently investigated (Schöbi and Sudret (2017)). In order to perform a reliability analysis, a large number of finite element realizations are usually required to obtain an accurate estimate of the probability of failure (Sudret (2017b)). To

mitigate the related computational cost, the complex FE model can be approximated by a meta-model (Marelli and Sudret (2014)). A prominent example of such a meta-model is the polynomial chaos expansion PCE which is based on a reasonable amount of FEM-calculated samples (e.g. training set). The construction of the meta-model, is a critical step in this approach, since the reliability of the uncertainty quantification directly depends on its quality.

In this paper, random fields are combined with meta-modelling to efficiently analyze quantities of interest in geotechnical problems. For this purpose, the uncertainty quantification Python based tool Adranis Sigma (2023)), is used. The documentation of Adranis Sigma is given by the Matlab-based software framework UQLab (Marelli and Sudret (2014)) which was developed by the same re-

search team. The approach is illustrated by evaluating the stability of a slope with a spatially variable friction angle. The probability of failure is assessed and compared to that obtained with a uniform friction angle field (where no spatial variability is taken into account). In addition, the influence of the correlation length on the failure probability is investigated.

## 2. RELIABILITY ANALYSIS USING META-MODELS

### 2.1. Monte-Carlo Simulation

A reliability analysis consists of estimating the probability that the system of interest will fail to meet a performance criterion (Sudret (2017b)). The behaviour of the system of interest is captured by a computational model such as the finite element model (FEM). This model maps a  $K$ - dimensional input vector  $\mathbf{U}$  to a output-space characterised by the quantity of interest (Schöbi and Sudret (2017)). In this case, the components of the input vector,  $\mathbf{u}_i$ , are uncertain and therefore associated to a probability density distribution (PDF)  $f_{U_i}$ . The failure probability  $P_f$  can thus be expressed as  $P_f = \mathbb{P}(\mathcal{M}(\mathbf{U}) \leq v_0)$ , where  $v_0$  is the performance criterion. It can also be represented by the following integral :

$$P_f = \int_{D_f} f_{\mathbf{U}}(\mathbf{u}) d\mathbf{u} \quad (1)$$

where  $D_f$  describes the failure domain, characterised by the set of realizations that do not meet the performance criterion. The integral in (1) cannot be solved analytically given the complex shape of  $D_f$  usually encountered in geotechnical systems. The failure probability  $P_f$  is thus estimated numerically by sampling-based approaches such as the Monte Carlo Simulation (Sudret (2017b)). The latter consists in simulating a large number of samples (here realizations of the uniform or random field) then carrying out a deterministic finite element analysis for each sample, and finally, statistically treating the response quantities of interest (Sudret (2017b)). Assuming a large number of samples of  $\mathbf{U}$ , the failure probability can be estimated by :

$$P_f = \frac{N_{Fail}}{N_{Tot}} \quad (2)$$

where  $N_{Fail}$  is the number of samples belonging to the failure domain  $D_f$  and  $N_{Tot}$  is the total number of samples (Schöbi and Sudret (2017)). Assuming that the failure probabilities follow a Bernoulli distribution, a number of  $\approx 4 \cdot 10^{k+2}$  samples are required in order to estimate accurately (with a coefficient of variation of  $\widehat{CV}_{P_f} = 5\%$ ) a probability of magnitude  $10^{-k}$  (Sudret (2017a)). Thus, reliability analysis becomes computationally expensive since the calculation model is complex. In such cases, a common approach is to approximate the computational model with a meta-model, such as the polynomial chaos expansion PCE, which is explained in the following chapter.

### 2.2. Polynomial chaos expansion PCE

One of the meta-modelling method is Polynomial chaos expansions (PCE) which approximates a computational model through its spectral representation with a sum of polynomial functions (Schöbi and Sudret (2017)). Its mathematical definition is as follows:

$$\mathcal{M}(\mathbf{U}) \approx \mathcal{M}^{PC}(\mathbf{U}) = \sum_{\alpha \in A} a_{\alpha} \psi_{\alpha}(\mathbf{U}) \quad (3)$$

where  $\psi_{\alpha}(\mathbf{U})$  are multivariate polynomials orthonormal with respect to the vector of the joint probability density function of the random independent input variables  $f_{\mathbf{U}}$ , and  $a_{\alpha} \in \mathbb{R}$  are the corresponding polynomial coefficients to indices  $\alpha$  in the truncated set  $A \in \mathbb{N}^K$  (Marelli and Sudret (2014)). The determination of the set of coefficients  $a_{\alpha}$  and the polynomial basis  $\psi_{\alpha}(\mathbf{U})$  is detailed in the UQLab user's manual for polynomial chaos expansions (Marelli and Sudret (2014)).

After the surrogate model is constructed, its predictive accuracy can be assessed by the leave-one-out (LOO) cross validation error  $\epsilon_{LOO}$ . This method is based on the concept of cross-validation which is developed in statistical learning theory (Marelli and Sudret (2014)).  $N$  meta-models  $\mathcal{M}^{PC}$  are constructed on a reduced experimental design set  $U \setminus u^{(i)}$ . A comparison is made between the PCE-based prediction on the excluded point  $u^{(i)}$  and the real value  $y^{(i)}$ . Thus, the leave-one-outcross-

validation error can be written as :

$$\epsilon_{LOO} = \frac{\sum_{i=1}^N (\mathcal{M}(\mathbf{u}^{(i)}) - \mathcal{M}^{PC\setminus i}(\mathbf{u}^{(i)}))^2}{\sum_{i=1}^N (\mathcal{M}(\mathbf{u}^{(i)}) - \hat{\mu}_Y)^2} \quad (4)$$

where  $\hat{\mu}_Y$  is the sample mean of the experimental design response (Marelli and Sudret (2014)). In section 5, the quality of the built surrogate models is given by its LOO-error.

### 3. SPATIAL VARIABILITY

#### 3.1. Random Fields

##### 3.1.1. Definition

To account for spatial variability, one can apply the theory of random fields. A random field  $H(x, \omega)$  is a set of random variables whose geographical location is given by the spatial variable  $x \in D_x$  and the associated outcome  $\omega \in \Omega$  in the space of elementary events (Schöbi and Sudret (2017)). A popular case of random fields is that of *Gaussian random fields*. It is entirely defined by the mean  $\mu(x)$ , standard deviation  $\sigma^2(x)$  and the auto-correlation function  $\rho(x, x' | l)$  with spatial correlation length  $l$ . The latter describes the distance over which properties tend to be spatially correlated (Schöbi and Sudret (2017)). In the random fields module of UQLab, the gaussian or squared exponential correlation function is implemented (Marelli and Sudret (2014)) and is consequently used in this article:

$$\rho(\tau_x, \tau_y; l_x, l_y) = \exp \left\{ -\frac{1}{2} \left( \frac{|\tau_x|}{l_x} \right)^2 - \frac{1}{2} \left( \frac{|\tau_y|}{l_y} \right)^2 \right\} \quad (5)$$

where  $(\tau_x, \tau_y) = (x_2 - x_1, y_2 - y_1)$ . The horizontal and vertical auto-correlation lengths  $l_x$  and  $l_y$  describe the distances within which the values are significantly correlated (Griffiths et al. (2011)). For simplicity, the following equations are expressed for a one-dimensional random field.

Random fields are represented numerically by a finite set of random variables employing stochastic discretisation methods (Schöbi and Sudret (2017)). The discretization methods reduce the dimensionality of the original random field and enable more tractable computations.

##### 3.1.2. Karhunen Loève Expansion

The continuous random field  $H(x, \omega)$  is discretized by a finite set of random variables via discretization methods to adapt it to computer applications. These methods aim to provide the best approximation using a minimal amount of random variables. Among the various techniques found in the literature, the Karhunen-Loève expansion is of particular interest here. It belongs to the family of series expansion methods, where the random field is represented as a finite series expansion of random variables and deterministic functions (Marelli and Sudret (2014)).

The Karhunen-Loève expansion of a random field  $H(x, \omega)$  is based on the spectral decomposition of its auto-covariance function  $C_{HH}(x_1, x_2) = \sigma(x_1)\sigma(x_2)\rho(x_1, x_2)$ , where  $\sigma(x_i)$  stands for standard deviation- and  $\rho(x_1, x_2)$  for the auto-correlation function of the random field. The auto-covariance function is generally bounded, symmetric and positive definite. Thus, the eigenvalue problem of the Fredholm integral equation defines the discretization of a random field based on a set of deterministic functions  $\varphi_i$  (Sudret and Kiureghian (November 2000)):

$$\forall i \in \mathbb{N}, \quad \int_{\Omega} C_{HH}(x_1, x_2) \varphi_i(x_2) dx_2 = \lambda_i \varphi_i(x_1) \quad (6)$$

where  $\lambda_i$  denotes the eigenvalues and the deterministic functions  $\varphi_i$  are the corresponding eigenvectors where  $\{\varphi_i\}_{i \in \mathbb{N}}$  form a complete orthogonal basis. The field  $H(x, \omega)$  can thus be completely defined by the following equation:

$$H(x, \omega) = \mu(x) + \sum_{i=1}^{+\infty} \sqrt{\lambda_i} \xi_i(\omega) \varphi_i(x) \quad (7)$$

In (7), the sequence  $(\xi_i(\omega))_{i \in \mathbb{N}}$  is a sequence of uncorrelated, zero-mean and unit-variance random variables (Sudret and Kiureghian (November 2000)). The eigenvalues are indexed in decreasing order (i.e.  $\lambda_1 \geq \lambda_2 \geq \dots \geq \lambda_M \geq \dots$ ). For practical application, the Karhunen-Loève expansion in equation (7) is truncated after a finite number of terms corresponding to the  $M$  largest eigenvalues (Marelli and Sudret (2014)):

$$H(x, \omega) \approx \widehat{H}(x, \omega) = \mu(x) + \sum_{i=1}^M \sqrt{\lambda_i} \xi_i(\omega) \varphi_i(x) \quad (8)$$

The accuracy of the approximation of the true random field  $H(x, \omega)$  by KL-expansion is linked to the number of terms  $M$  to keep in the expansion in (8). It can be assessed through the so-called "energy" ratio or explained variance (Marelli and Sudret (2014)):

$$\sum_{i=1}^M \lambda_i / \sum_{i=1}^{\infty} \lambda_i \geq \delta_e \quad (9)$$

where  $\delta_e$  corresponds to a given threshold. In this article,  $M$  is computed based on a target explained variance of  $\delta_e = 99\%$ . The required number of terms  $M$  in order to fulfil the condition in (9) depends on the correlation length  $l_x$  (and  $l_y$  in bi-dimensional case) in the correlation function  $\rho(\cdot)$  (defined in Eq.(5)). The greater the correlation length, the less variant the random field is, the lower the expansion term  $M$ .

The reduced dimensionality, enables the construction of surrogate models. The independent standard KL coefficients of a Gaussian random field  $((\xi_i(\omega))_{i \in \mathbb{N}}$  in equation 7) can be transformed from the normal to the physical space via an isoprobabilistic transformation and given as an input to the finite element model  $\mathcal{M}$ .

#### 4. WORKFLOW

The procedure applied in this study to perform reliability analysis on a slope's stability is illustrated in figure 1. The left side of the figure, includes all steps which are performed using the finite element software ZSOIL (2020). In this part of the approach, a finite element model of the considered slope is created with the mean values of the soil properties. All relevant information, such as the finite element mesh and the boundary conditions, are stored in a ZSOIL input file. The right side represents the steps followed in the probabilistic approach using the uncertainty quantification tool Adranis Sigma (2023). The white arrow boxes between the two sides depict the coupling between the approaches, permitting the reliability analysis.

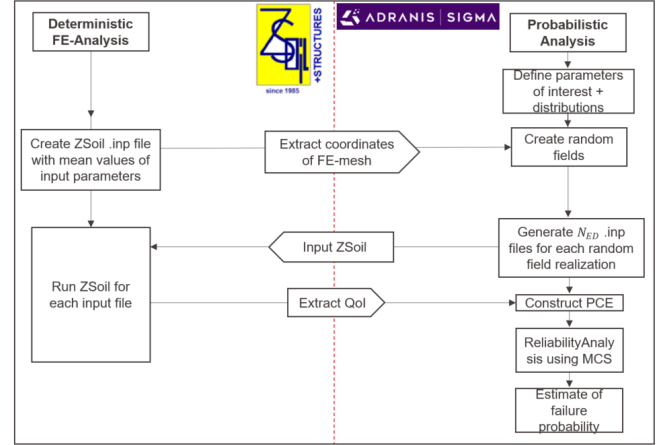


Figure 1: Flowchart of applied procedure to perform slope reliability analysis with the finite element software ZSOIL (2020) and the uncertainty quantification tool Adranis Sigma (2023). QoI: quantity of interest

The first step in the probabilistic analysis is to identify the uncertain input parameters along with their distributions and statistical moments. To create the random fields, the coordinates of the centroids  $(x_{c,i}, y_{c,i})$  of each element  $i = 1, 2, \dots, n_{elem}$  ( $n_{elem}$  being the total number of elements in the FE-mesh) are extracted. An independent standard normal sample matrix of dimension  $N_{ED} \times M$  is generated. The matrix is then transformed to the physical, correlated space and  $N_{ED}$  ZSOIL input files are created with different soil properties for each element. These samples are further evaluated by the finite element model and the quantities of interest (QoI) are extracted. A PCE is constructed on the basis of the computed samples and finally the failure probability is given through a Monte-Carlo Simulation.

#### 5. SLOPE RELIABILITY ANALYSIS CONSIDERING SPATIALLY VARIABLE FRICTION ANGLE

##### 5.1. Problem statement

To illustrate the combination of meta-model and random fields for reliability analysis, the stability of a slope under constant rainfall is studied. The slope's geometry and its finite element model are shown in figure 2. The slope's inclination is  $\beta = 30^\circ$ . The mesh is built with a total of  $n_{elem} = 725$  Q4 elements (4 nodes per rectangular element, linear shape functions). Rainfall is simulated as an inflow

boundary condition  $q(t)$ , which is defined from the associated load function, defined as follows:

Time [h]	$q(t)$ [m/h]
0	0
4	0.012
200	0.012

Table 1: Load function associated with rainfall inflow

The boundary conditions are given in solid terms (displacements and tractions represented in red in figure 2) and in fluid terms (pressures and fluxes represented in purple in figure 2). Displacements are fixed at the bottom and restrained horizontally on the edges. A groundwater table is considered three meters below edge  $\overline{BC}$ . On the surface, seepage elements control the inflow of the rain. The 2-phase boundary problem is solved via a transient analysis using the finite element software ZSOIL (2020). The constitutive model is non associated Mohr-Coulomb and the safety factor SF of the slope is assessed via a  $\tan(\phi) - c$  reduction algorithm.

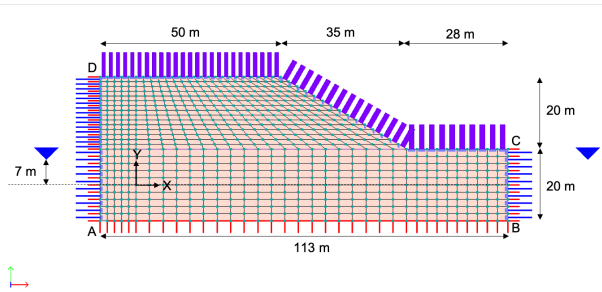


Figure 2: Finite element mesh and boundary conditions of the studied slope ( $n_{elem} = 725$ ,  $l_{elem,x,min} = 2m$ ,  $l_{elem,y,min} = 1.3m$ )

First, a deterministic analysis of the slope with the parameters given in table 2 is performed, where the mean value of the friction angle is considered. The uncertainty related to the friction angle is taken into account in a second step and discussed in the next section. The stability of the slope is evaluated via the safety factor (SF) calculated after 100h of rain and gives 1.125. The created mechanism is represented in figure 3.

$U_i$	Distribution	$\mu$	CoV
$E$	Constant	100 MPa	-
$\nu$	Constant	0.3	-
$\gamma$	Constant	14.2 kN/ms	-
$e_0$	Constant	0.9	-
$\phi$	<b>Gaussian</b>	<b>20°</b>	<b>10 %</b>
$c$	Constant	10 kN/m <sup>2</sup>	-
$\psi$	Constant	0°	-
$k_x = k_y$	Constant	0.05 m/h	-
$\alpha$	Constant	1 1/m	-
$S_r$	Constant	0	-

Table 2: Input parameters with given mean ( $\mu$ ) and coefficient of variation (CoV), where  $E$ : Young's modulus,  $\nu$ : Poisson's ratio,  $\gamma$ : Unit weight,  $e_0$ : initial void ratio,  $\phi$ : friction angle,  $c$ : cohesion,  $\psi$ : dilatancy angle,  $k_x, k_y$ : Darcy's coefficient,  $\alpha$ : saturation constant

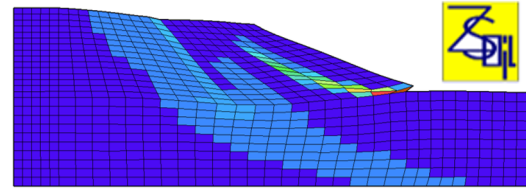


Figure 3: Failure mechanism of the slope with mean input parameters with SF = 1.125 at  $t=100h$ . Warm colours represent shear zones.

## 5.2. Meta-modelling

In this section the reliability of the slope given in figure 2 is analysed employing the polynomial chaos expansion PCE and accounting for spatial variability of the friction angle  $\phi$ . In particular we are interested in the evaluation of the safety factor SF of the slope after 100 hours of rainfall with intensity given in table 1. Failure occurs when  $SF \leq 1$ . Thus the resulting failure probability is  $P_f = \mathbb{P}(\mathcal{M}(\mathbf{U}) \leq 1)$ . Two gaussian random field analysis are examined, where the friction angle's mean is  $\mu_\phi = 20^\circ$  and its standard deviation  $\sigma_\phi = 2^\circ$  (see table 2). One represents a heterogenous field by rather short correlation lengths in both directions  $l_x = 8 m$  and  $l_y = 8 m$ . The other one simulates a horizontal stratigraphy with correlation lengths  $l_x = 10^3 m$  and  $l_y = 8 m$ . Both cases are illustrated in figure 4.

Both random fields are discretized with the

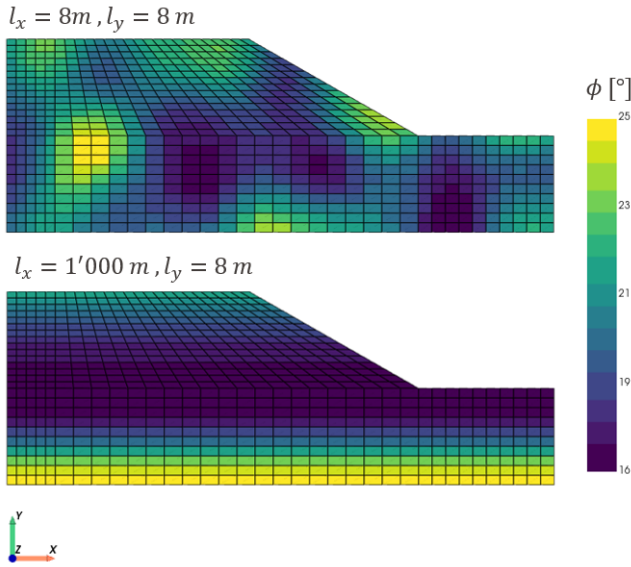


Figure 4: Exemplary random field realizations for a heterogeneous field with  $l_x = 8 \text{ m}$ ,  $l_y = 8 \text{ m}$  and a horizontal stratification field with  $l_x = 10^3 \text{ m}$ ,  $l_y = 8 \text{ m}$

Karhunen-Loève algorithm. To account for more than 99 % of the variability of the random field, a different number of terms  $M$  in the KL expansion (see Eq. 8) must be retained for the types of random fields:

$l_x$ [m]	$l_y$ [m]	$M$
8	8	64
$10^3$	8	5

Table 3: Karhunen-Loève expansion order  $M$  in function of the correlation lengths  $l_x$  and  $l_y$

Since the heterogeneous random field represents greater variability, a higher expansion order  $M$  is required to capture its variability. Figure 5 illustrates the convergence of the explained variance (or energy ratio, see Eq. 9) with increasing number of terms  $M$ . At  $M = 64$  an energy ratio of 99.99 % is achieved, which is considered sufficient.

The number of terms required in the KL-expansion also represents the number of uncorrelated random variables  $\xi_i(\omega)_{i \in \mathbb{N}}$ ,  $i = 1 \dots M$ . This means, that  $M$  input marginals with zero-mean and unit-variance gaussian distributions are used to create the probabilistic input model of the PCE. The surrogate model is built on  $N_{ED} = 10 \times M$  crude

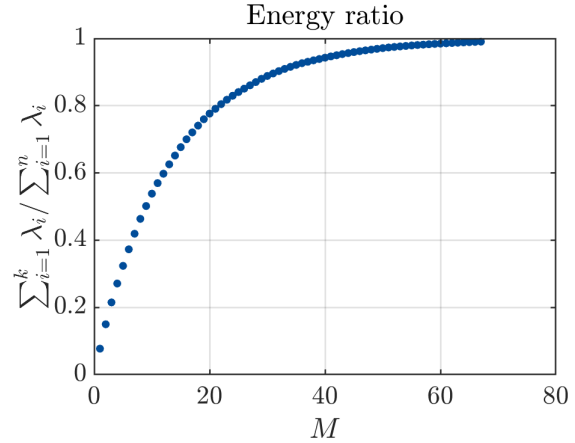


Figure 5: Eigenvalues of the correlation matrix up to the expansion order for  $M = 64$  (example for heterogeneous random field with  $l_x = 8 \text{ m}$ ,  $l_y = 8 \text{ m}$ )

Monte Carlo samples ( $N_{ED}$  is the size of the experimental design), which, according to the authors, gives a satisfactory quality. This implies that  $N_{ED} = 640$  and  $N_{ED} = 50$  samples were evaluated with the finite element model  $\mathcal{M}$  for the heterogeneous and horizontally layered random field respectively. For the uniform friction angle field, where no spatial variability is taken into account,  $N_{ED} = 50$  samples are computed. The convergence of the quality measure of the PCE, the leave-one-out error  $\epsilon_{LOO}$ , with increasing number of samples is illustrated in figure 6 for the case of a heterogeneous random field with  $l_x = l_y = 8 \text{ m}$ .

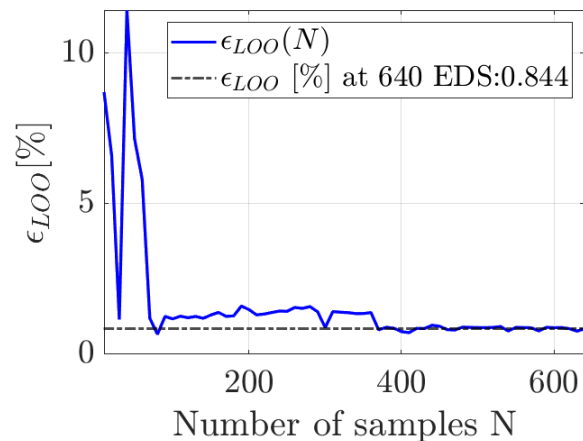


Figure 6: Convergence of the leave-one-out error  $\epsilon_{LOO}$  with increasing size of samples  $N$

With  $N_{ED} = 640$  a leave-one-out error of  $\epsilon_{LOO} =$



0.844% is achieved, which is considered sufficient. Generally, for geotechnical applications a LOO-error of  $\epsilon_{LOO} \leq 2\%$  is considered acceptable. After figure 6, already 80 samples seem to be quite enough to reach the performance criterion. To illustrate the difference between the prediction performance of a PCE created with  $N_{ED} = 60$  and one with  $N_{ED} = 80$ , their prediction  $Y^{PCE}$  is plotted against the true value  $Y^{ZSOIL}$  in figure 7 in red and in blue respectively.

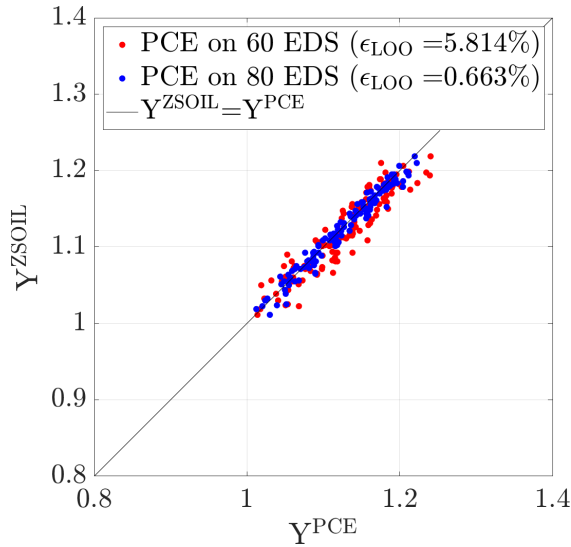


Figure 7: PCE Validation for heterogenous random field ( $l_x = 8\text{ m}, l_y = 8\text{ m}$ ): red dots represent the values found with a PCE created with 60 EDS, blue dots represent the values found with a PCE created with 80 EDS

The closer the points are to the line, the better the prediction of the meta-model. Since the blue points are fairly aligned with the line, the quality of the PCE created with only  $N_{ED} = 80$  is considered acceptable. For the sake of consistency, the results presented in the following section are based on the PCE constructed with  $N_{ED} = 10 \times M$  for the corresponding random field realisations.

### 5.2.1. Failure probabilities

The failure probabilities for the heterogenous, the horizontal and uniform random field realizations are obtained by a Monte-Carlo Simulation with  $n_{MC} = 10^6$  samples based on their corresponding PCEs. The accuracy of each built PCE is given by its LOO-error and is reported in table 4. The

probability density function (PDF) of the safety factor is illustrated in figure 8, where the red curve represents the horizontal layered random field, the blue one the heterogenous random field and the black one a uniform field where no spatial variability is modelled. The difference between the uniform field and the spatially variable fields as well as the influence of the choice of auto-correlation lengths for the random field is clearly visible.

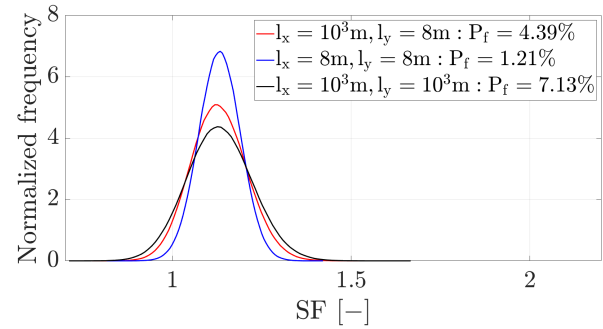


Figure 8: Probability density function PDF of the safety factor SF of the slope for the heterogenous random field in blue, for the horizontal layered random field in red and for the uniform field in black

The black curve, representing the uniform friction angle field, is wider than the two curves obtained with spatially variable friction angle with a larger area in the failure domain. The failure probability is consequently larger as well. Comparing the horizontal and heterogenous random field, the red curve is wider than the blue curve, with a greater extension in the failure domain, resulting in a higher probability of failure. This observation can be explained by taking a closer look to the exemplary random fields shown in figure 4. The dark blue elements represent areas where the friction angle is rather low. In the case of a horizontal stratigraphy, possible large zones with low shear-strength can be modelled close to the surface, which facilitates a mechanism. Whereas for a heterogenous field, low-friction elements are more likely to be distributed in such a way as to inhibit the development of a continuous shear band over which a mechanism can take place. Table 4 summarises the determined failure probabilities for the two random field cases considered as well as a third case for a uniform friction angle field. The uniform field is

simulated by taking large correlation lengths such as  $l_x = 10^3$  m and  $l_y = 10^3$  m.

$l_x$ [m]	$l_y$ [m]	$P_f(t = 100h)$ [%]	$\epsilon_{LOO}$ [%]
8	8	1.21	0.84
$10^3$	8	4.39	0.38
$10^3$	$10^3$	7.13	0.41

Table 4: Comparison between the PCE based (accuracy given by  $\epsilon_{LOO}$ ) failure probabilities evaluated for the two random field configurations and a homogeneous friction angle field

The comparison of the established failure probabilities shows the great influence of the different approaches to simulate the spatial variability and uncertainty of the friction angle. Assuming a uniform field, where all the soil parameters are the same in space, worst case scenarios are more likely to take place and could lead to an overestimation of the failure probability. Taking account of the spatial variability of mechanical properties, is more realistic and thus leads to more reasonable results. However, the choice of the random field parameters such as the correlation lengths, have a great impact of the estimated failure probabilities and must be taken prudently.

## 6. CONCLUSION

The reliability of a slope under constant rainfall is analysed by combining the finite element software ZSOIL and the uncertainty quantification tool Adranis Sigma. In particular the friction angle is modelled by random fields. Three different correlation structures of the friction angle field are studied by varying the correlation lengths. The resulting failure probabilities are compared. For the studied example, it can be concluded that the failure probability tends to decrease when taking into account a spatially varying friction angle. The probabilistic analysis is efficiently performed with the help of meta-models like the polynomial chaos expansion. The purpose is to not only render reliability analysis, applied to geotechnical engineering problems more realistic by the means of random fields, but also to demonstrate the possibility of applying it in everyday practice.

## 7. ACKNOWLEDGEMENTS

The authors would particularly like to thank Marc Gros Lambert and Samuel Kivell for their support and advice throughout the project.

## 8. REFERENCES

- Griffiths, D.V., Huang, J., Fenton, G.A., 2011. Probabilistic infinite slope analysis. *Computers and Geotechnics* 38, 577–584. URL: <https://www.sciencedirect.com/science/article/pii/S0266352X11000474>, doi:10.1016/j.compgeo.2011.03.006.
- Marelli, S., Sudret, B., 2014. UQLab: A Framework for Uncertainty Quantification in Matlab, 2554–2563 URL: <https://ascelibrary.org/doi/10.1061/9780784413609.257>, doi:10.1061/9780784413609.257. publisher: American Society of Civil Engineers.
- Schöbi, R., Sudret, B., 2017. Application of conditional random fields and sparse polynomial chaos expansions in structural reliability analysis URL: <http://hdl.handle.net/20.500.11850/237463>, doi:10.3929/ETHZ-B-000237463. medium: application/pdf Publisher: ETH Zurich.
- Sigma, A., 2023. version 0.1.0. Adranis GmbH, Switzerland.
- Sudret, B., 2017a. Lecture Notes on Structural Reliability and risk analysis.
- Sudret, B., 2017b. Stochastic Finite Element Methods and Reliability A State-of-the-Art Report .
- Sudret, B., Kiureghian, A.D., November 2000. Stochastic finite element methods and reliability a state-of-the-art report. *Structural Engineering, Mechanics and Materials 5th Int*, 18–21. URL: <https://ethz.ch/content/dam/ethz/special-interest/baug/ibk/risk-safety-and-uncertainty-dam/publications/reports/SFE-report-Sudret.pdf>.
- ZSOIL, 2020. A Windows-Based Tool offering a unified approach to numerical simulation of soil and rock mechanics, above & underground structures, excavations, soil-structure interaction and underground flow, including dynamics, thermal and moisture migration analysis.